Journal of Structural Geology, Vol. 7, No. 6, pp. 623 to 636, 1985
Printed in Great Britain

0191-8141/85 $03.00 + 0.00

Horizontal cleavage in southeastern Sinai: the case for a coaxial strain history

ARTHUR P. S. REYMER*

Institute of Earth Sciences, Department of Geology, The Hebrew University of Jerusalem, Israel

and

GERHARD OERTEL

Department of Earth and Space Sciences, University of California, Los Angeles, CA 90024, U.S.A.

(*Received* 28 *September* 1984; *accepted in revised form* 13 *March* 1985)

Abstract—A horizontal cleavage and associated lineation are developed in a low-pressure igneous-related metamorphic terrain in southeastern Sinai. The cleavage is axial planar to recumbent folds, which are never large, and varies from a smooth slaty cleavage to a discrete crenulation cleavage. Structural evidence on the macro, meso and microscales suggests that cleavage and lineation were formed during irrotational extension and not by simple shear. Estimates of strain using the March method indicate 50–70% vertical shortening. This structural evidence when combined with metamorphic and age data strongly suggests that the cleavage was formed by the forceful emplacement of a pluton at depth.

INTRODUCTION

CLEAVAGE is harder to explain by 'compressive forces' if it dips gently than if it is steeply inclined or vertical. In collision or Alpine-type orogenic belts, gently dipping cleavage is now commonly taken to be the effect of large-scale simple shear deformation. Such cleavage is usually axial planar with respect to asymmetric, tight to isoclinal, recumbent folds and nearly parallel to thrusts and nappe boundaries (e.g. Mattauer 1975). Subhorizontal cleavage may, however, be formed by listric normal faults curving at depth towards subhorizontal and grading into diffuse zones of ductile deformation (e.g. Mattauer 1975, Sibson 1983). Above forcefully intruding plutons or gneiss diapirs extension has been shown to form a subhorizontal to gently dipping cleavage (e.g. Dixon 1975, Sylvester *et al.* 1978). There the deformation is irrotational, and the area of cleavage formation is restricted to the roof region of the diapir, although a swarm of such bodies may underlie a large area.

The present study is concerned with the local development of a subhorizontal cleavage in a part of an orogenic belt not characterized by Alpine-type collision tectonics. Folds in the Arabian Shield, in Sinai, and elsewhere are predominantly upright, metamorphism indicates low pressure, and igneous intrusions are abundant. We will show that subhorizontal cleavage in the Wadi Kid area of the Sinai Peninsula could have formed by irrotational strain due to horizontal extension. Structural and metamorphic data will be combined to justify a model of folding and cleavage caused by the forceful emplacement of a pluton at depth. Although the postulated diapir cannot be directly observed, its presence would explain several seemingly separate or even contradictory observed features.

TECTONIC EVOLUTION OF THE WADI KID METAMORPHIC COMPLEX

The following summary is based on detailed mapping, facilitated by good desert exposures, of several key areas in the Wadi Kid metamorphic complex in southeastern Sinai (Fig. 1) (Reymer 1983, Reymer & Yogev 1983, Gaber 1983, Navon & Reymer 1984) and on studies of its tectonic and thermal evolution (Bielski 1982, Reymer *et al.* 1984a, Reymer 1985). We restrict this summary to features relevant for the present study.

The Wadi Kid Group (Shimron 1980) developed from protoliths divisible into a clastic shallow-marine succession and an overlying subaerial volcanic sequence. The clastics have been deposited in a slowly subsiding basin probably floored by continental crust, as revealed by the occurrence of granitic pebbles in the Kid Group, dated at about 750 Ma (Priem *et al.* 1984), and by evidence that the rocks were deposited not far below or above sea level. The crust was therefore probably at least 20 km thick before deposition of the Kid Group. Horizontal shortening folded the Kid Group into large upright E–W to NE–SW trending folds (D_1) with an associated S_1 axial plane slaty cleavage (Fig. 2). The latter is, however, not everywhere clearly distinguishable from bedding lamination. No convincing field evidence for regional important reverse faults or thrusts associated with D_1 have been found by us, but such structures have been

* Current address: Department of Marine, Earth and Atmospheric Sciences, North Carolina State University, Raleigh, NC 27965-8208, U.S.A.

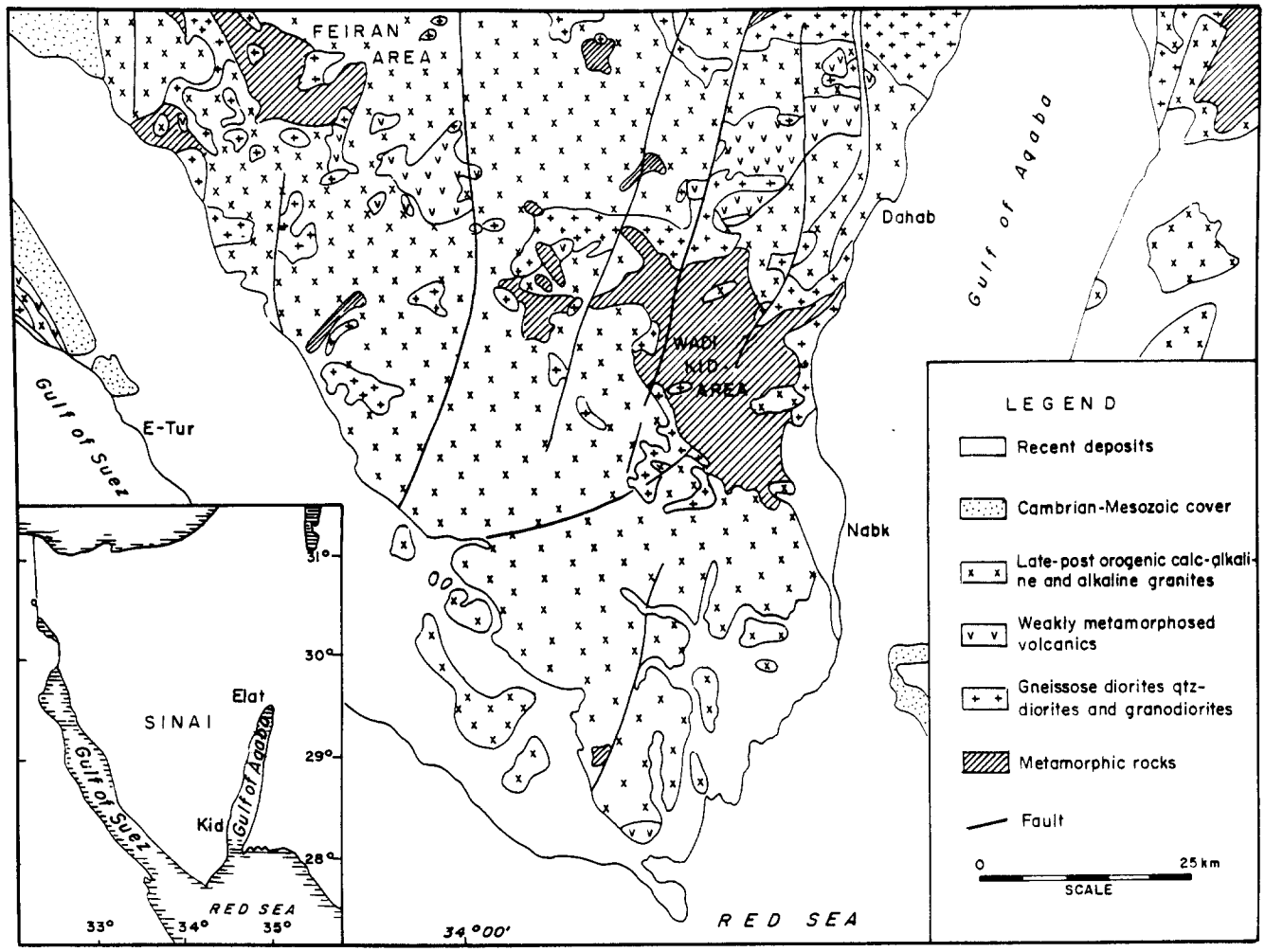

Fig. 1. Location and general geological setting of the Wadi Kid area.

observed locally (Shimron 1983, 1984). On the other hand, a décollement zone caused by this phase of deformation almost certainly exists at deeper levels. Strong N–S shortening is also recorded in the Elat area, some 150 km north of Wadi Kid, where thrusting and folding produced an inverted metamorphic sequence (Reymer *et al.* 1984b and in prep.).

Deposition and D_1 folding must have occurred in the time span bracketed by a basement age of 750 Ma and that of a phase of major granitic plutonism and felsic volcanism, dated at 600–550 Ma, and commonly designated as the Pan-African event. The oldest volcanics of the Kid group are probably associated with a phase of plutonism at approximately 650 Ma. The folding (D_1) thus seems to have followed very soon after this event, and volcanism and plutonism continued into and until the end of the Pan-African event. A second deformation phase (D_2) occurred while the area was being metamorphosed to a grade up to amphibolite facies under pressures of about 300 MPa (Reymer *et al.* 1984a). Rb–Sr whole-rock ages of metasediments and metavolcanics and K–Ar mica ages of about 600 Ma indicate that this last 'tectonothermal' event was contemporaneous, within the dating uncertainties, with the major phase of volcanism and granite intrusion (Halpern & Tristan 1981, Bielski 1982, Reymer & Steinitz, unpubl. results). This D_2 deformation phase is the subject of our present study. Usually weak later folding and kinking (D_3) about various axes occurred during cooling of the area. A schematic cross-section is shown in Fig. 2.

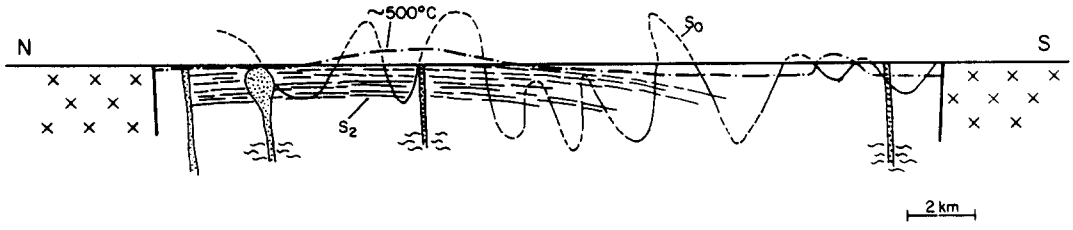

Fig. 2. Schematic N–S cross-section through Wadi Kid area showing F_1 folds, S_2 cleavage; approximate trace of the boundary between greenschist and amphibolite facies, shown as the 500°C isotherm; metamorphic felsic dikes and their inferred source (Reymer 1985).

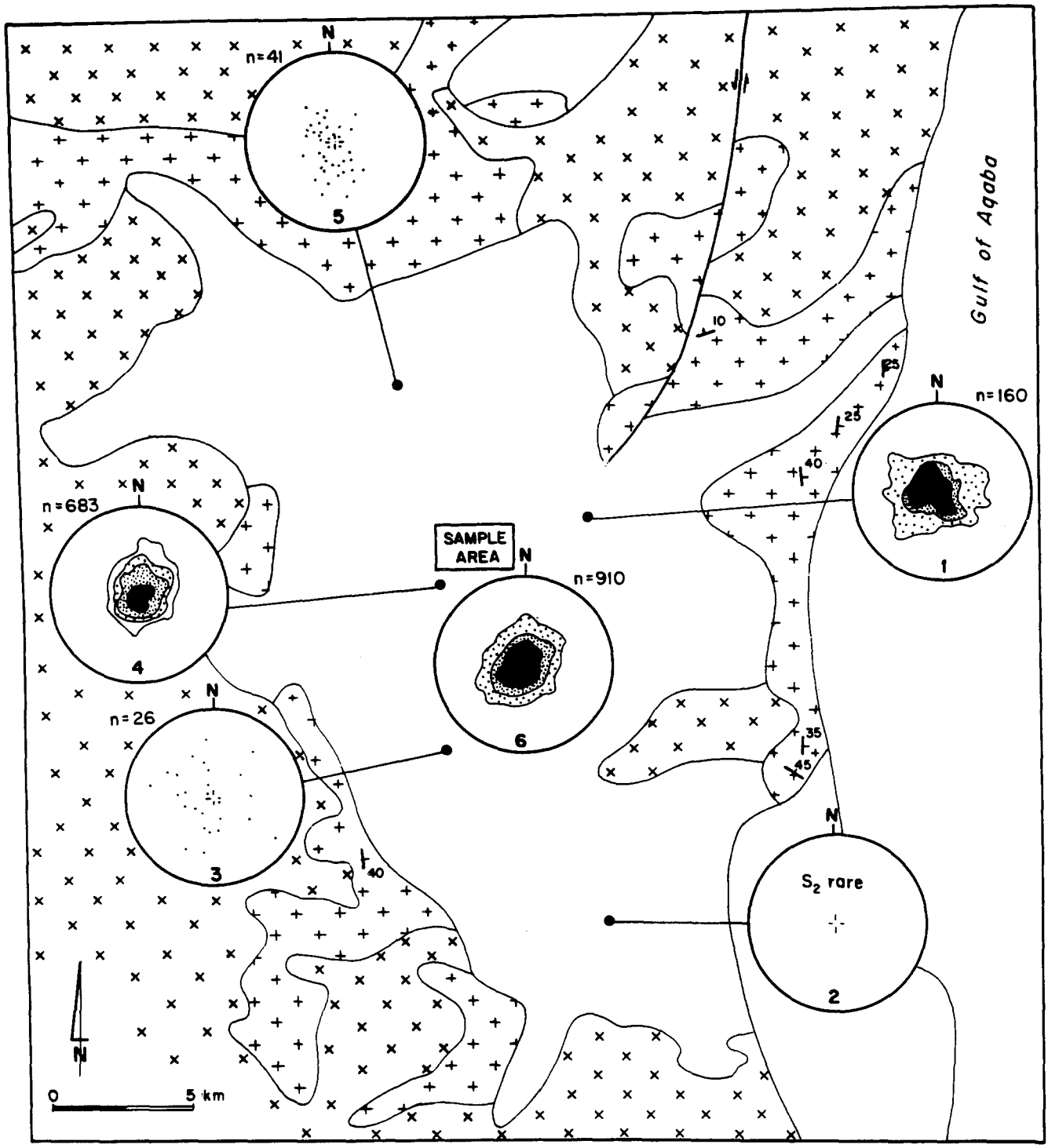

Fig. 3. Orientation of cleavage (S_2) in the Wadi Kid area. Data were collected in domains with a radius of about 6 km indicated by the attached dot. Diagram 6 represents 1–5 combined. Contours 1, 3, 5, and >10% per 1% area. Equal area projection 3 after Gaber (1983); 5, after Navon & Reymer (1984). Lower hemisphere. For legend see Fig. 1.

STRUCTURAL DATA

The second deformation phase produced an S_2 cleavage axial-planar to recumbent, open to tight folds that refold the steep limbs of F_1 folds. Individual folds are non-cylindrical on the meter scale and have near-horizontal hinges. A mineral lineation is statistically parallel to F_2 hinges but may noticeably deviate from parallelism in individual folds. In the southern part of the Wadi Kid area, F_2 folds are also present, but have an axial- plane cleavage only locally in the form of an incipient crenulation cleavage (Reymer & Yogev 1983). The folds there are much less regular, often intrastratal, and commonly far from cylindrical.

The S_2 cleavage varies from penetrative (slaty) to crenulation cleavage. The regional orientation is shown in Fig. 3 and is near-horizontal on average. Most of its scatter results from F_3 folding.

Stretching lineations are defined by the preferred orientation of inequant minerals, stretched mineral

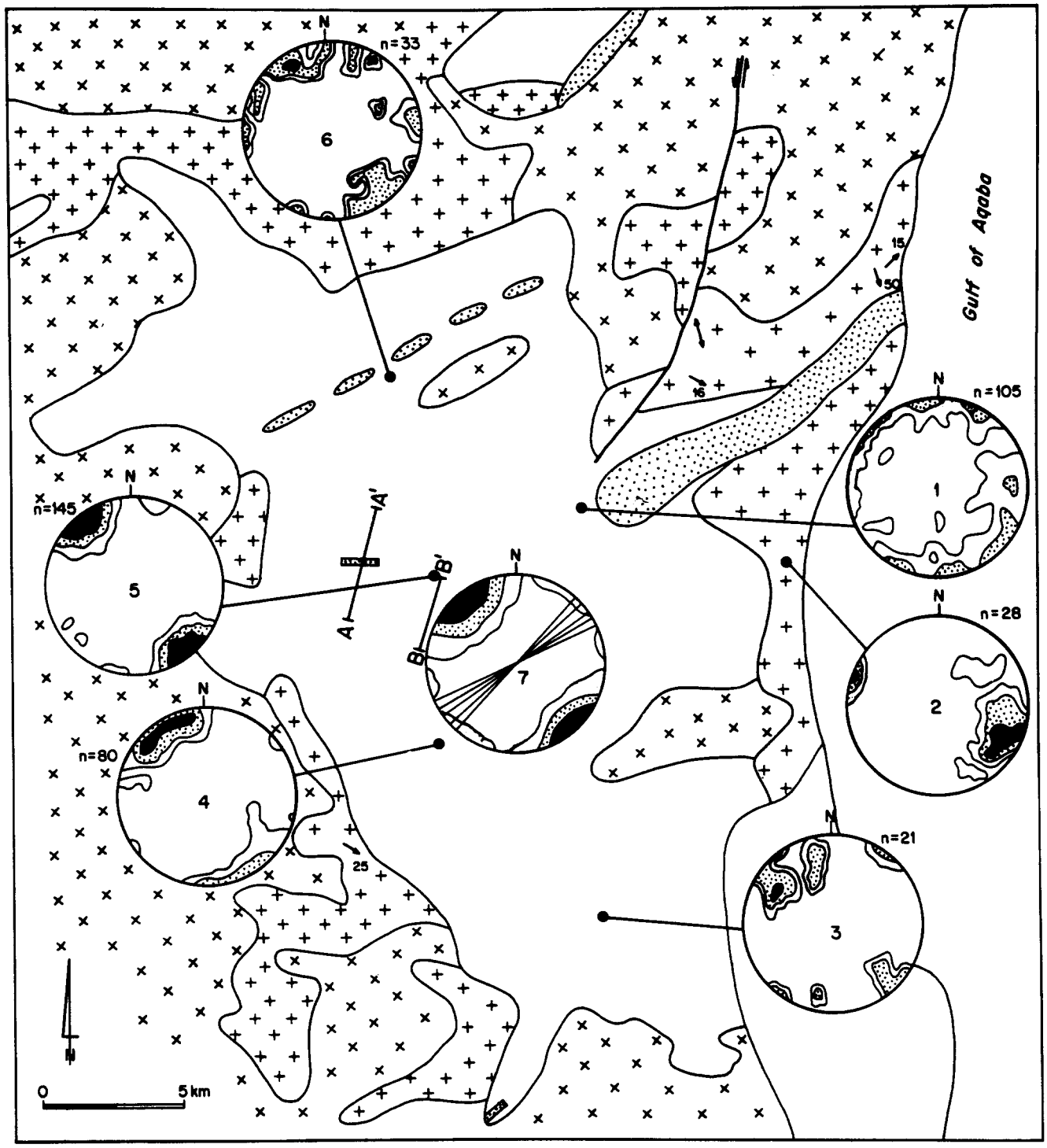

Fig. 4. Orientation of mineral lineation in the Wadi Kid area (from Reymer 1985). For equal-area diagrams 1–6 see explanation, Fig. 3. Diagram 7 represents 1–6 combined. Contours 1, 3 and >5% per 1% area. Stippled, syntectonic and synmetamorphic felsic dikes are of anatectic origin. Equal-area projection 3 is after Reymer & Yogev (1983); 4, after Gaber (1983); 5, after Navon & Reymer (1984). Lower hemisphere. A–A′ and B–B′ locations of cross-sections of Fig. 5.

aggregates and long axes of deformed pebbles in conglomerates. A lineation map (Fig. 4) shows that, apart from local variations, the dominant mineral or pebble lineation in the area is oriented NW–SE. Reymer (1985) shows that a set of metamorphic felsic dikes intruded almost perpendicularly to the NW-trending lineation during D_2. These dikes bear aluminum silicates and are most likely the result of high-grade metamorphism and anatexis at depth. The clustering of its directions notwithstanding, lineation is not penetrative on every scale; locally it can be weak or absent.

Most of the granodioritic–dioritic plutons which border the Wadi Kid area possess both a foliation and a lineation. The foliation dips commonly more steeply in the plutons than in the country rocks, but the lineation usually passes into the plutons without refraction.

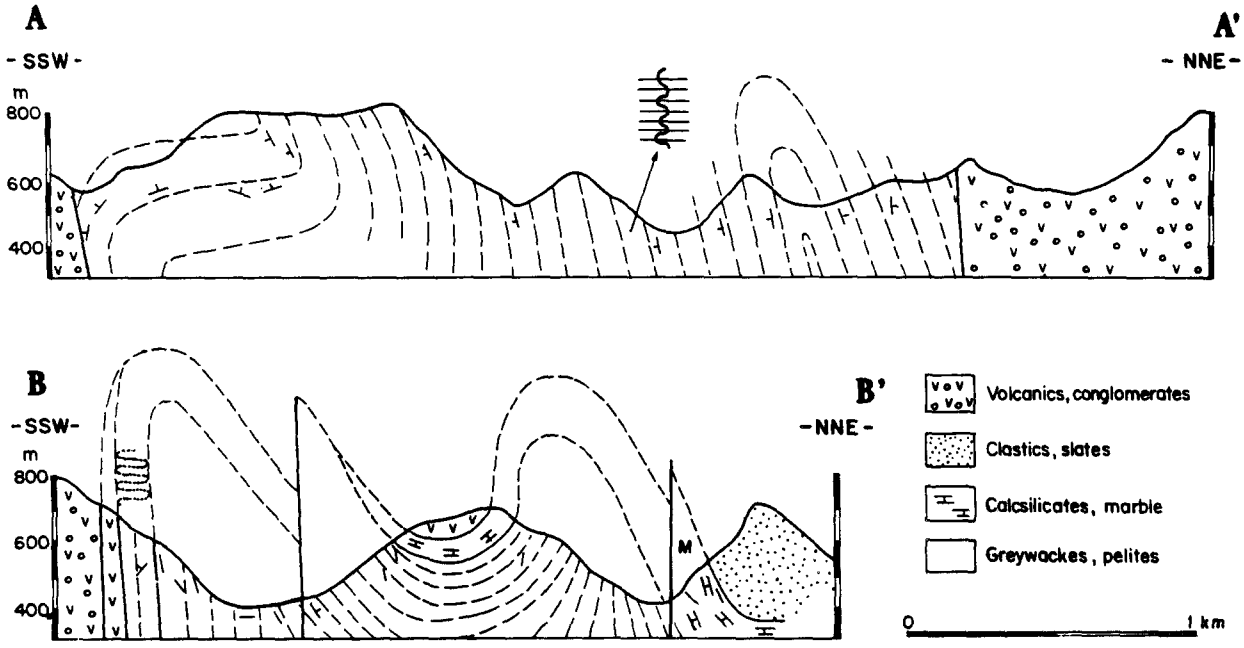

Fig. 5. Two parallel cross-sections through the central part of the Wadi Kid area (after Navon & Reymer, 1984) demonstrating F_1 folding on a large scale. Location shown in Fig. 4. Bedding traces represent enveloping surfaces of open to tight F_2 folds, except at the F_1 hinges. Beds younging toward ticks. M, location of marble horizon on Fig. 13.

EVIDENCE FOR D_2 IRROTATIONAL EXTENSION

The most obvious evidence against large-scale simple shear as a cause for the formation of the S_2 cleavage formation is the bedding attitude. In the southern half of the area, where the D_2 overprint is moderate or weak, bedding is steep or vertical except at the F_1 hinges. In the central and northern parts, information about the orientation of bedding on the large scale can only be abstracted from confusing local detail by careful mapping; a typical cross-section resulting from such mapping (Navon & Reymer 1984) is shown in Fig. 5. The generalized bedding planes shown in this section are actually the traces of enveloping surfaces of F_2 folds. Thus to the center and north of the area, F_1 axial planes are not rotated with respect to those in the south, although they are strongly overprinted by F_2. This assessment is confirmed by the close match in stratigraphic sequence between the southern and central areas (Navon & Reymer 1984), which limits possible regional correlations to an overall synformal F_1 structure (Reymer 1983). Thus, F_2 folds are fairly small (maximum several meters amplitude), and the intensity of the D_2 deformation causing them rapidly increases northwards and is thus quite local.

The metamorphic felsic dikes, mentioned before and shown on Fig. 4, were intruded during the D_2 deformation as shown by internal F_2 folds, foliation, and lineation but have not been rotated into low-dip attitudes parallel to S_2 (Reymer 1985). The dikes must therefore have been intruded during the later stages of the D_2 deformation episode, when country rock began to react brittly to continued extension. Complementary evidence on the microscale follows below.

The main metamorphic minerals, biotite, garnet, andalusite and staurolite, grew between the episodes of D_1 and D_2, although the peak of metamorphism has been determined as later than D_2 (Reymer *et al.* 1984a, Navon & Reymer 1984). Because the slightly dome-shaped metamorphic zone boundaries are not disrupted, no major horizontal displacements seem to have occurred during D_2. This argument is especially strong because the metamorphism indicates low pressure and high temperature with narrow metamorphic zones; if important displacements had occurred after growth of the various porphyroblasts, they should be conspicuous.

On the intermediate scale, the deformation history can be seen to have followed a complex path. Interpretation of the deformation path is constrained by the general absence of asymmetry in the F_2 folds. Because fairly symmetric folds can theoretically develop during certain stages of progressive simple shear, fold symmetry by itself is only a weak argument against regional simple shearing; it becomes valid, however, in combination with arguments from observations on the macroscale.

Rotation, folding, and boudinage of sills, dikes and quartz veins are common in the area, but have not been analyzed systematically.

Considerations from the macroscale constrain us to regard the deformation history as having been, in general, an irrotational, horizontal extension; we can now investigate whether the observed microstructures are compatible with these results. For the sake of discussion, we postulate a simple D_2 history in three stages: a probable initial homogeneous, finite shortening (D_{2a}) of the vertical layers followed by buckling (D_{2b}); third, after the buckle folds were strongly appressed, there was renewed homogeneous vertical shortening (D_{2c}).

During the second stage (D_{2b}), strain in the fold limbs must have accumulated as a series of non-coaxial strain increments. Evidence for this is preserved in the angle between inclusion patterns in porphyroblasts (Rosenfeld 1968) representing S_1 and/or S_0, and the external S_2 cleavage (Figs. 6a–c). The maximum measured angles are about 110°, but most of the 40 measurements lie between 60 and 90°. Such rotations can be expected during the development of an axial-plane crenulation cleavage (Williams & Schoneveld 1981).

Fold hinge domains probably continued their strain history with a deformation more or less coaxial with that of the first stage. Crenulation cleavage in the hinges can be expected to be at about 90° to the inclusion patterns, and the porphyroblasts not to rotate. These expectations are confirmed by observation.

In the third stage, advancing strain should have produced further extension parallel to cleavage, and the deformation (D_{2c}) should, once again, have become essentially coaxial in all domains. In many localities, crenulation cleavage should at this stage be transformed into schistosity (cf. Williams & Schoneveld 1981, p. 329). Third-stage strain increments were only insignificantly overprinted by D_3, and therefore many microstructures can with certainty be assigned to stage D_{2c}.

Figure 6(d) shows a detail of a biotite fabric, with two old grains in conjugate orientations, both probably slipped on (001), and a strong cleavage defined by new biotite grains. In general these biotite fabrics are very similar to those described by Manktelow (1979) (see also Navon & Reymer 1984). The absence of indicators of a particular shear sense suggests a coaxial strain path. Figure 7(a) shows strain shadows developed around ilmenite grains, suggesting dissolution and redeposition of quartz. The strain shadows do not indicate any rotation. Figure 7(b) shows a fractured and pulled apart garnet crystal with quartz filling the void. The garnet fragments also have not been rotated. Figure 8 shows several generations of extensional quartz veins. The older veins were refolded during subsequent strain increments and the quartz is flattened parallel to cleavage. Veins rotated into parallelism with the cleavage underwent boudinage during continued strain. Such vein systems are predominantly found in fine-grained micaceous rocks and amphibole-rich schists. The latter contain numerous veins made up of pale amphibole and/or epidote which show varying degrees of refolding about horizontal axes. All these veins reflect brittle–ductile behavior under progressive extension parallel to the cleavage in conjuction with solution and redeposition. None of the above fabrics indicate simple shear, although by themselves they do not eliminate the possibility of simple shear.

A good example of the D_2 deformation history at various scales is given by the structures in a marble horizon, which forms an important stratigraphic marker in the central Wadi Kid area (Fig. 9). A system of stylolites and extensional microfaults postdates tight F_2 folds and indicates that the maximum compressive stress (σ_3) was vertical, and the least compressive stress (σ_1) horizontal. Structures on all scales in this example indicate vertical shortening and horizontal extension.

The progressive deformation outlined above took place under progressively higher temperatures. A good example of the microstructural evidence for such a thermal/structural history is the inclusion of 'early' biotite porphyroblasts in 'later' andalusite porphyroblasts (Fig. 6a). Progressive temperature increase probably caused strain-softening during the D_2 deformation, perhaps enhanced by strong fluid activity and metamorphic reactions. However, this may not be true during the later stages of the deformation, as will be discussed below.

STRAIN

Preferred orientation of phyllosilicates in samples from central Wadi Kid were measured, using a method described by Oertel (1981) and Wenk (1985). The validity of using the intensities of preferred orientations of micas as a measure of strain following March's (1932) method was recently reviewed by Oertel (1983, 1985a,b).

Two sets of samples were investigated. The first set was collected from an exposure of metarhyolite, which contained a micaceous zone. The second set was chosen from a collection of samples of slates a few hundred meters away from the first set (sample area framed on Fig. 3).

The mica-rich zone within the metarhyolite from which the first set of samples (S0–5) are derived was initially regarded as a shear zone of major (Shimron 1983, 1984) or minor significance (Reymer & Oertel 1982). However, subsequent detailed work showed that the subhorizontal S_2 cleavage cuts undeflected through this mica-rich zone into quite massive rhyolite, and therefore cannot be related to shear across this 30° S-dipping zone. Whether this mica-rich zone amid much more massive rhyolite represents an older shear zone, a paleoweathering horizon and/or a fracture acting as a conduit for hydrothermal solutions is not clear. A brief description of the mica fabrics within this zone is given below.

Outside the mica-rich zone the metarhyolite is massive, with spots of plagioclase grains. Fine-grained (10 μm) muscovite defines a subhorizontal cleavage. Within the mica-rich zone, the cleavage is defined by mica films which curve around plagioclase phenocrysts. In quartz-feldspar domains, muscovite grains at a high angle to the cleavage occur throughout the zone. Quartz has a fairly constant grain size of 10–30 μm. At some places, rocks occur with 60–70% muscovite. In such samples, the mica fabric defines a discrete crenulation cleavage. Quartz-bearing microlithons are about 100 μm wide and contain muscovite grains at a high angle to the cleavage. Such grains are often bent and kinked and show signs of pressure solution. Quartz veins occur throughout the rock, and many are folded with the rock cleavage lying in the axial plane. This observation is in

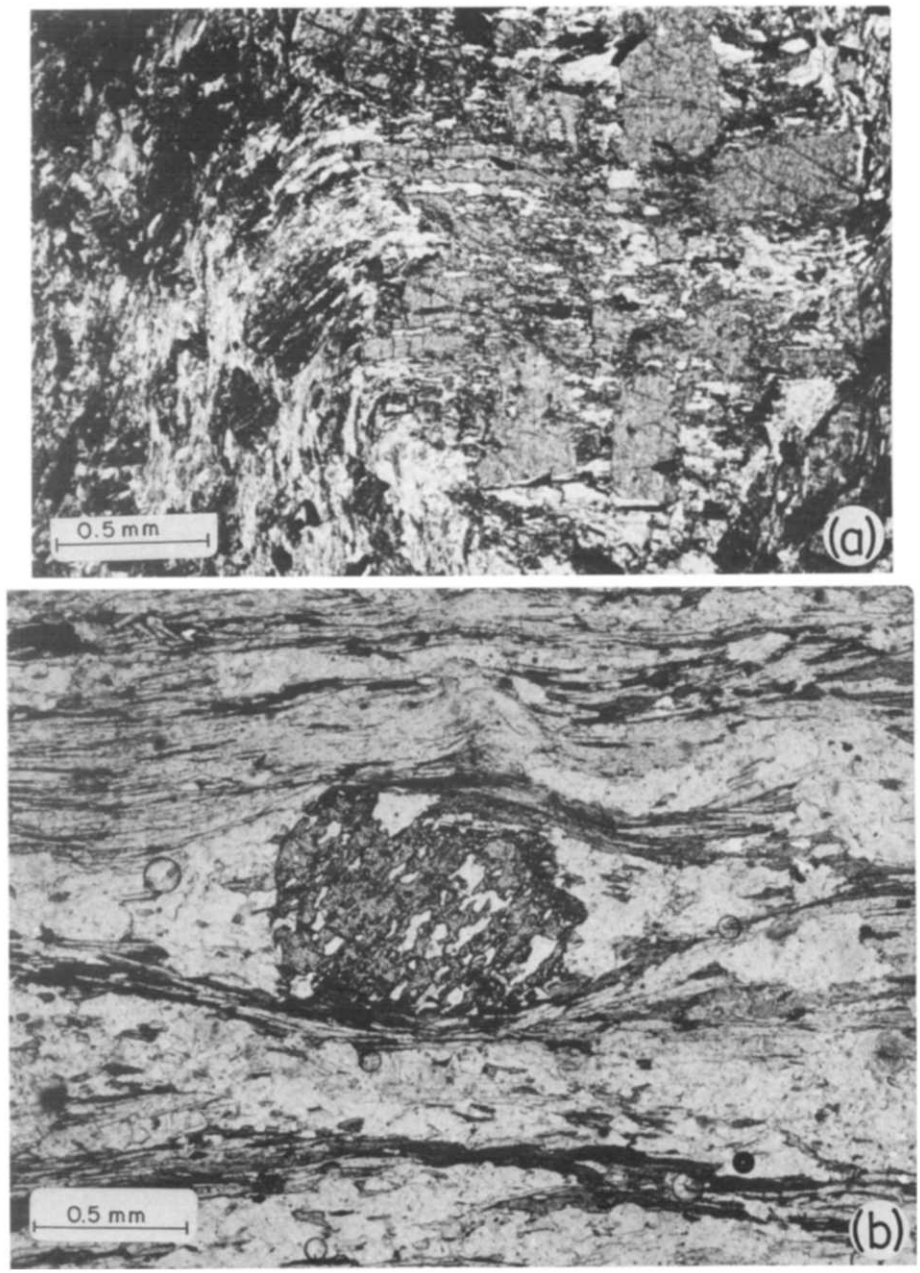

Fig. 6. (a) Large andalusite crystal with included earlier grains defining inside schistosity, S_i, perpendicular to outside schistosity, S_e. Note also biotite porphyroblasts predating andalusite growth and rotation. (b) Garnet porphyroblast with S_i at 45° to S_e. Note also evidence of garnet dissolution at the contacts with the mica domains. Strain shadows postdate rotation.

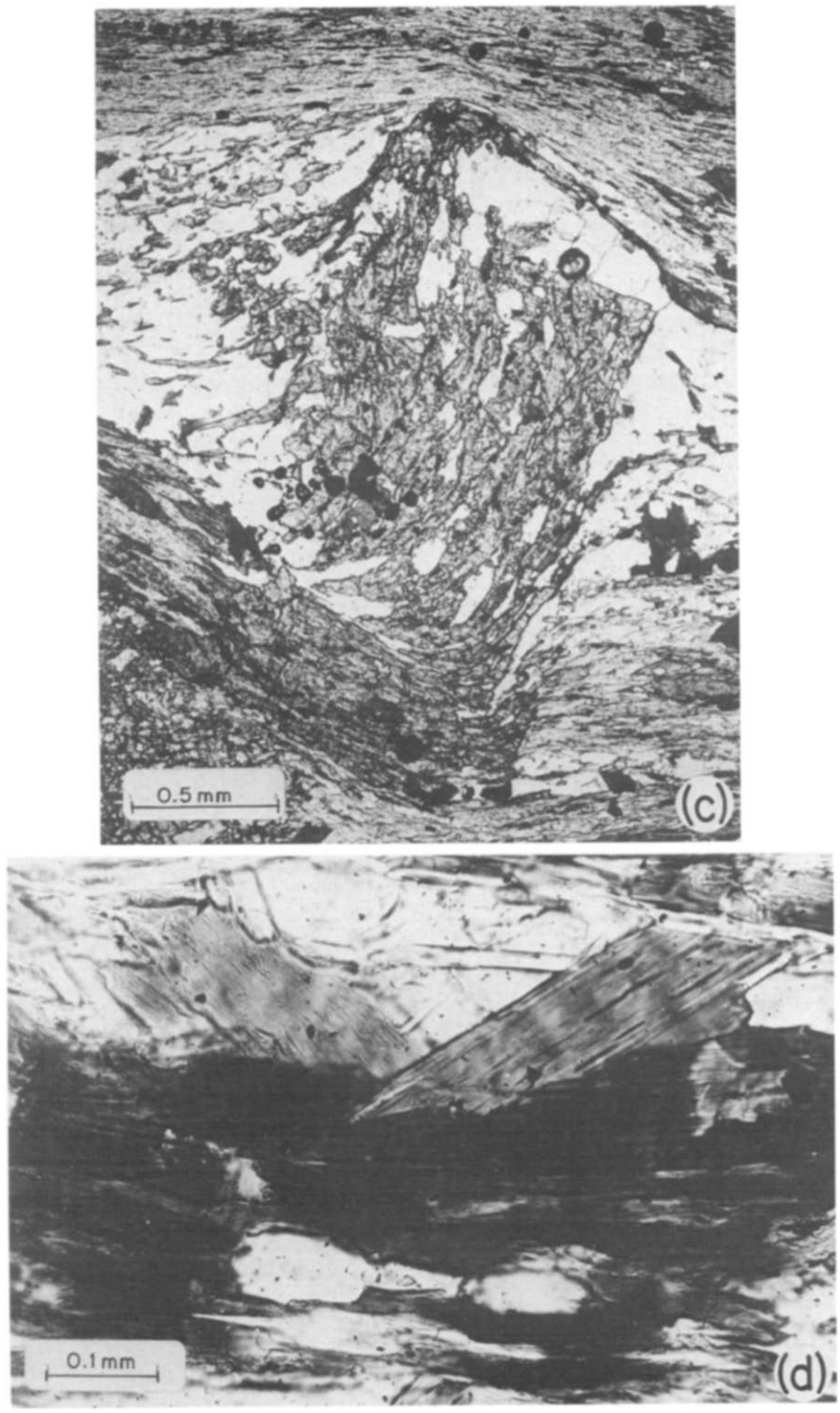

Fig. 6. (contd) (c) Andalusite crystal showing growth pre-, syn-, and post-F_2, tracking part of the deformation history. Rotation about 60°. (d) 'Old' biotite grains suggesting slip on (001) and 'new' grains defining S_2.

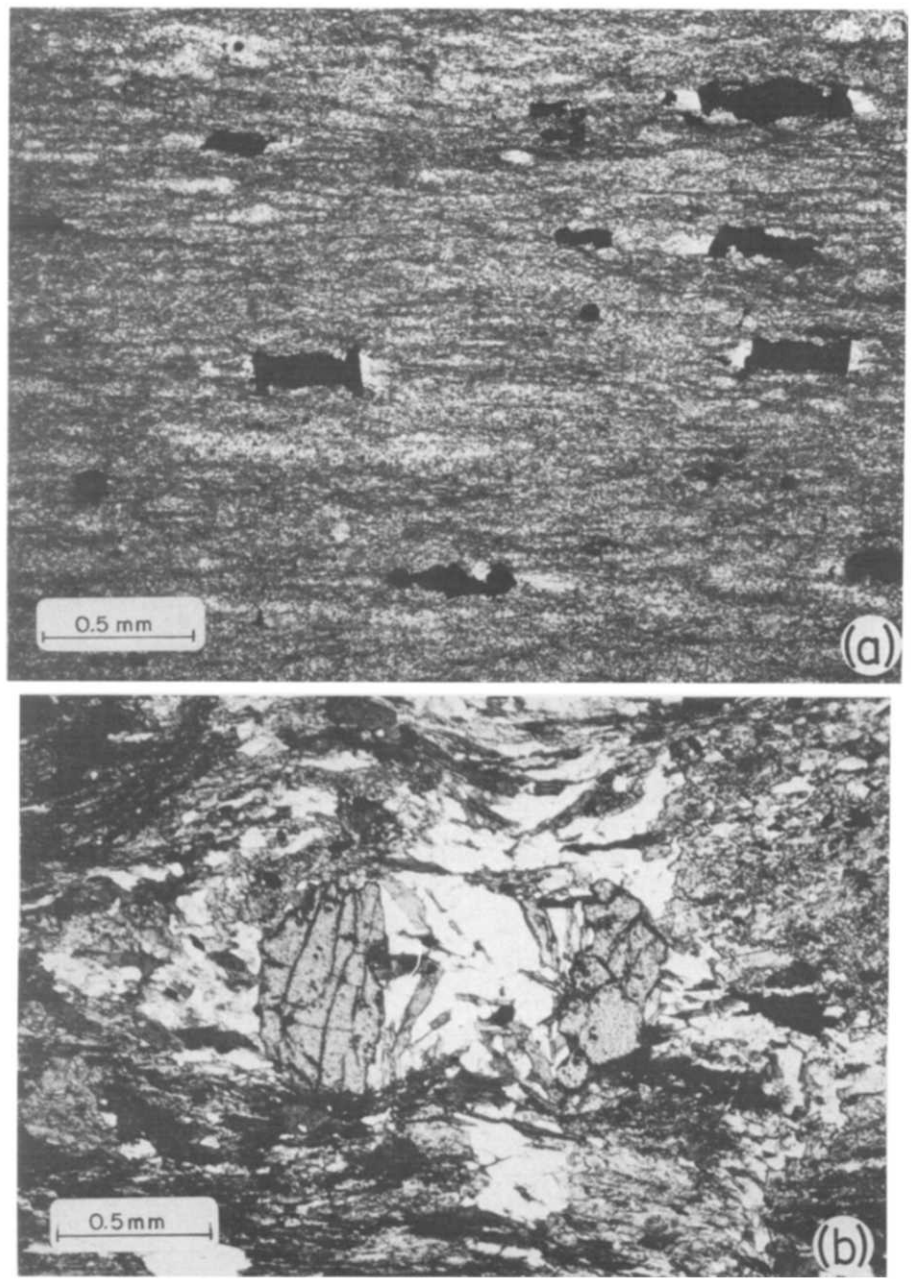

Fig. 7. (a) Strain shadows around ilmenite grains, showing no sign of rotation. (b) Boudinaged garnet crystal with quartz infilling and weak strain shadows.

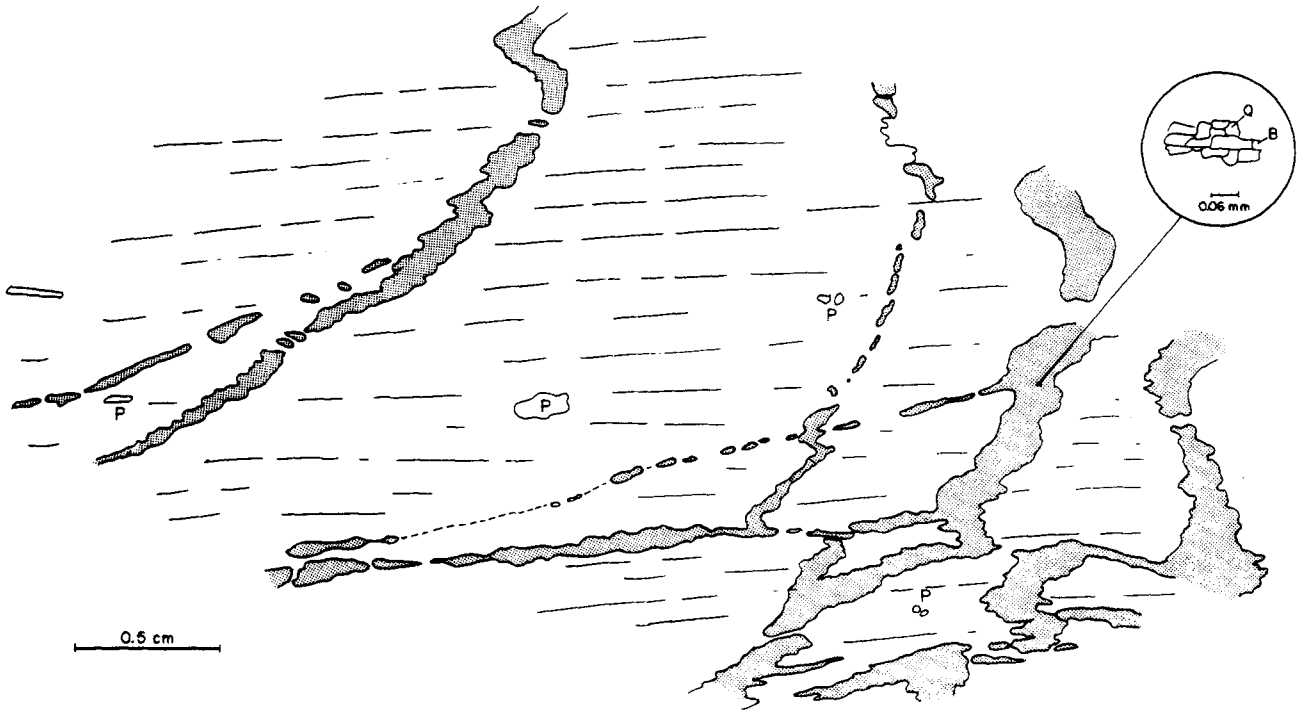

Fig. 8. Tuffaceous slate, central Wadi Kid area. System of quartz veins due to progressive extension parallel to cleavage, brittle failure, and subsequent ductile deformation. Depending on orientation, veinlets are folded or boudinaged. Vein quartz shows preferred shape orientation parallel to cleavage. Q, quartz; B, foliation consisting of biotite and opaque material; P, boudinaged or fractured plagioclase crystals.

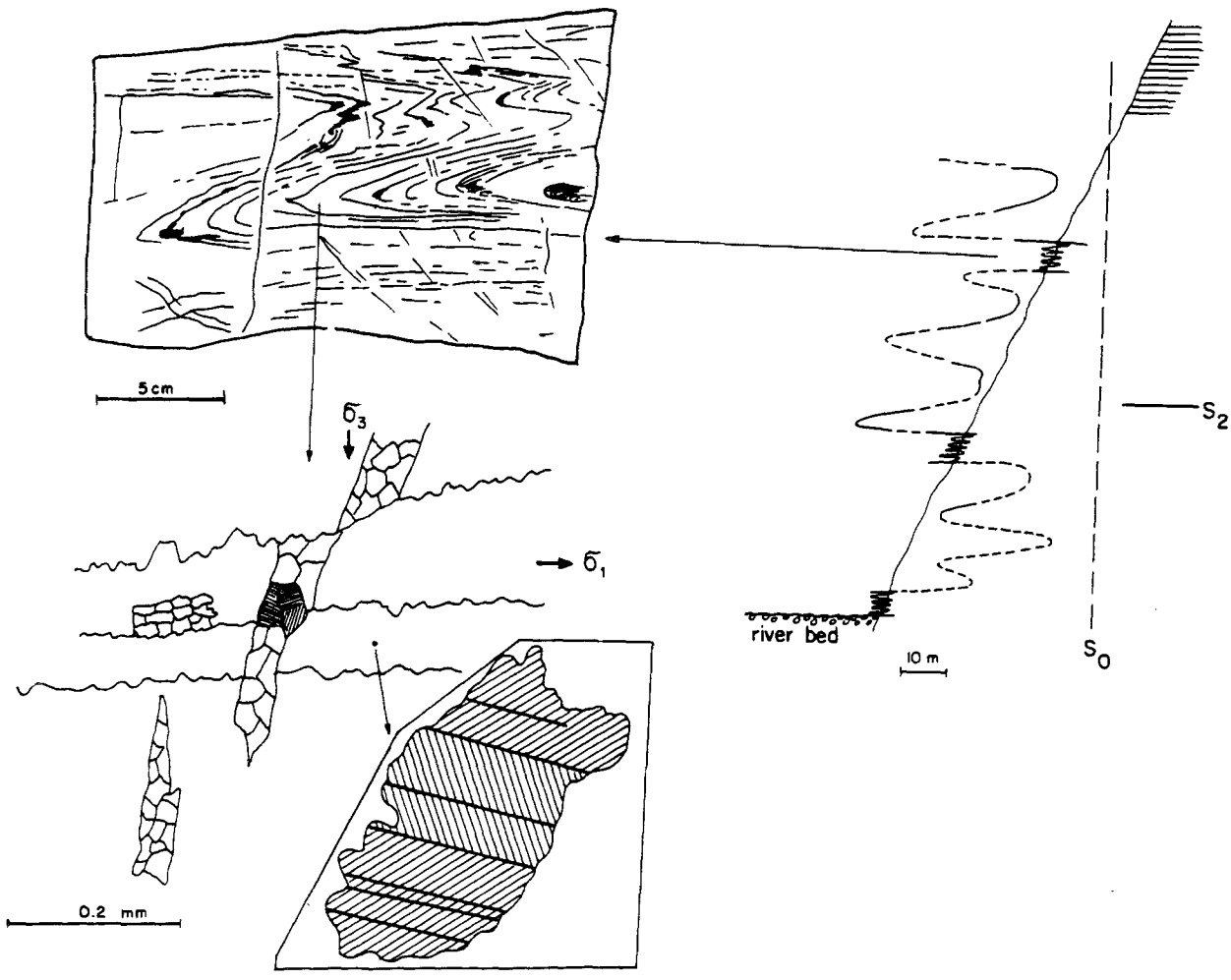

Fig. 9. Macro-microscale features in marble layer exposed in northern slope of Wadi Madsus, central Wadi Kid area (see Fig. 5 for location). Reconstruction of macroscale folding of marble layer based on known fold style, exposures and known orientation of bedding (S_0) from other units. Note scales and consistency of observations of the various scales, indicating a history of pure shear.

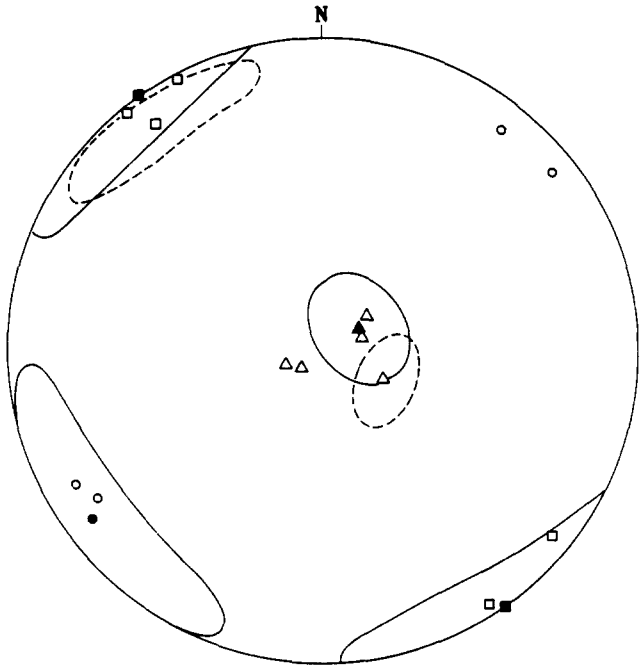

Fig. 10. Equal-area projection of measured mica preferred orientations in samples from central Wadi Kid area. Filled and open symbols refer to sample sets 1 (S0-5) and 2 (samples with prefix R), respectively. From sample set 1 the means and 1σ (solid closed curves) are plotted, from set 2 all individual measurements. Triangles, poles of maximum mica orientation; circles, intermediate; squares, minimum mica orientation. Dashed ovals, outer limits of poles to cleavage (near the center) and lineation (near the primitive circle).

line with those described above and indicates simultaneous brittle extension and ductile deformation. The general strain-free nature of all constituent minerals points to annealing and recovery after deformation ceased. This is in agreement with the assessment that metamorphism outlasted D_2 deformation in the central Wadi Kid area (Reymer 1983, Reymer *et al.* 1984a).

The second set of samples includes slates with very fine-grained muscovite and biotite. In sample R-582 pseudomorphs of cordierite are present. Sample R-620 contains the system of quartz veins discussed above and shown in Fig. 8. Scattered large grains of plagioclase and sometimes quartz suggest a tuffaceous origin for these slates.

The decision to measure preferred orientation in the second set of samples was made after the field area became inaccessible to us. We, therefore, had no oriented samples and had to rely exclusively on internal markers, the mesoscopically evident foliation and lineation in the specimens. Fortunately (Figs. 3 and 4), these features have a consistent orientation throughout the area, and because of the near-parallelism of the principal strain directions and the mesoscopic markers, the potential misorientation from turning specimens upside-down did not introduce ambiguities of orientation. Lack of absolute orientation data, however, prevented us from quantitatively estimating the degree of scatter of the observed preferred orientation and from calculating and stating the mean strain of the sampled domain.

The results of X-ray goniometer measurements are given in Table 1 and plotted on an equal-area projection in Fig. 10. The distribution of maximum, intermediate, and minimum concentrations of poles to (001) corresponds closely to the mesoscopic orientation of cleavage and lineation in the sample area (Figs. 3 and 4). In Table 1, intensities of preferred orientation of mica are translated into strains according to the theory of March (1932). Vertical shortening strains of 50–70% were measured. These values have to be taken as minimum values. We interpret them as mainly D_2 strains, because of poor S_1 development and (re)crystallization after D_1 concurrent with prograde metamorphism. It is also clear that not all strains are plane. Sample R-216 lies well within the flattening field of strain, and R-620 also deviates from plane strain. The quartz veins of the latter sample (Fig. 8) indicate extension parallel to cleavage, but perpendicular to the trend of the mineral lineation, and therefore also indicate non-plane strain.

Table 1. Strain measurements

Specimen no.	Mica	Orientations of principal axes* ϵ_1	ϵ_2	ϵ_3	Principal March intensities† ρ_i			Principal strains‡ ϵ_i		
S-0										
S-1										
S-2										
S-3	mus	(144,00)	(234,11)	(055,79)	[0.17	0.49	12.6]	[0.80	0.30	−0.60]
S-4										
S-5										
R-140	mus/bio	(137,01)	(047,07)	(229,84)	[0.06	0.61	27.3]	[1.50	0.18	−0.67]
R-216	mus/bio	(330,05)	(060,09)	(211,80)	[0.18	0.38	14.8]	[0.78	0.39	−0.59]
R-582	mus/bio	(126,01)	(217,11)	(026,79)	[0.19	0.67	7.9]	[0.74	0.14	−0.50]
R-620	mus/bio	(312,02)	(222,15)	(047,75)	[0.13	0.56	14.3]	[1.00	0.21	−0.59]

* Orientation given as (trend, plunge).
† Measured intensity/mean intensity.
‡ Assuming constant volume.

INTERPRETATION AND DISCUSSION

The overall irrotational extension postulated above for the development of cleavage and lineation during the D_2 folding episode can be explained if this deformation phase represents the effects of a forcefully emplaced pluton below the present erosion level. Ramsay (1975) coined the name 'balloon tectonics' for this type of deformation (cf. Holder 1979). However, most plutons actually seem to have intruded in an asymmetric way, guided by local weaknesses in the country rock during final emplacement, and foliation and lineation may therefore form patterns that are far from concentric (e.g. Guillet *et al.* 1983). This also applies to Wadi Kid, where lineations (Fig. 4) do not follow a concentric pattern.

Body forces resulting directly from gravity (gravitational 'collapse') may have assisted in the initial buckling of steep beds but cannot be responsible for all of the D_2 strain. Gravitational collapse alone cannot explain continuing horizontal extension after the cleavage was already in existence. It has been shown, both experimentally and theoretically (Dixon 1975, Schwerdtner *et al.* 1978, Morgan 1980) as well as in natural examples (Nelson *et al.* 1977, Sylvester *et al.* 1978, Schwerdtner *et al.* 1978, 1983, Davidson 1980, Soula 1982, Torske 1982, Rattey & Sanderson 1984), that large irrotational horizontal extensions occur above the crests of rising diapirs (whether mantled gneiss domes or plutons), especially late during their emplacement. Large strains may accumulate (Dixon 1975) and even mylonites can be formed (Wilson 1983). In this context, the irregularity and weakness of F_2 folding and virtual absence of S_2 cleavage in the southern area in contrast to the central and northern areas of Wadi Kid can be explained by greater distance from the inferred pluton. This inference is consistent with the lower metamorphic grade (subtracting later contact metamorphic overprints) but, lacking strain estimates from the south, cannot be confirmed by quantitative arguments. Alternatively, a regional extensional strain field was present, on which the contact strain discussed in this study was a (strong) overprint. Some support for the existence of such a residual strain field comes from the foliated diorites (Figs. 3 and 4). The E-dipping foliation within these plutons seems to preclude a direct relationship with D_2. However, lineation in these bodies is generally concordant with the lineation in the country rocks. This indicates that NW–SE extension was present before and after D_2, as based on field relationships between the plutons and the metamorphic rocks. In any case, horizontal extension should replace the somewhat different interpretation of Reymer & Yogev (1983) for D_2 in the southern Wadi Kid.

Mapping of metamorphic zones, examination of phase equilibria, and geothermobarometry show that the Kid complex contains gently-dipping metamorphic zones, which reached 300 MPa and 565°C in the central area (Reymer 1983, Reymer *et al.* 1984a). Thus, the metamorphic and structural dome apices coincide (Fig. 2). Reymer *et al.* (1984a) invoke a magmatic heat source for the metamorphic pattern and the steep geothermal gradient. This interpretation is consistent with that based on structural data in this study.

According to evidence on the macroscale (dikes) and microscale (microfaults), deformation mechanisms progressively changed from ductile to partly brittle. This seemingly contradicts the observation that the thermal peak occurred just after D_2 (Reymer *et al.* 1984a, Navon & Reymer 1984). Several factors may have played a role. (1) Metamorphic dehydration may have been essentially completed before D_2, and dryness may have embrittled the hotter rocks during the late stages of the deformation history, depressing the brittle–ductile transition zone to deeper levels. (2) After rotating the steep bedding to subhorizontal (on the finest scale), further extension may have acted along the bedding and cleavage-parallel stiffest direction of the anisotropic rock. Rocks are relatively prone to fracture under tensile (or effectively tensile) loads, especially if they are anisotropic and the load acts parallel to a direction of greatest stiffness. (3) Strain rate may have been higher during the late stages. These explanatory factors do not mutually exclude each other and could have been active in various combinations.

Because the area is bordered on three sides by intrusive bodies (Fig. 1) not enough is known about strain outside the area to allow discussion of compatibility with larger-scale strain patterns.

CONCLUSIONS

A subhorizontal cleavage in the Wadi Kid area was probably formed by protracted irrotational extension. Such a deformation regime could exist above a forcefully intruding diapiric pluton. This kinematic conclusion is corroborated by a coeval thermal pulse and age determinations of plutonism and metamorphism, indicating that the latter two events occurred almost at the same time.

Alternatively, a general crustal extension could have produced the folds and horizontal cleavage in the Wadi Kid area. However, this interpretation would require the thermal peak during D_2 to be coincidental.

Erosion seems not yet to have unroofed the pluton we consider responsible for the strain; it could lie as little as 2 km below the present surface (Reymer 1985). Vertical shortening of at least 50 and possibly 70% in the overlying rocks coincided with prograde metamorphism, and the rocks reacted mainly in a ductile manner; at some stage, however, brittle fracturing also became important.

Acknowledgements—A.R. is particularly grateful to Ami Yogev and Oded Navon, whose detailed mapping, partly carried out during the desert summer to meet the April 1982 deadline when the Sinai Peninsula became inaccessible from Israel, contributed in no small measure to the results of this study. Thanks are also due to Alan Matthews for discussions and support. The comments by two anonymous reviewers and Peter Hudleston substantially improved the manuscript. A grant from the Batsheva de Rothschild Fund is gratefully acknowledged. G.O.'s measurements were performed with support from the National Science Foundation, Grant EAR 80-07444.

REFERENCES

Bielski, M. 1982. Stages in the evolution of the Sinai Peninsula. Unpublished Ph.D. thesis, The Hebrew University of Jerusalem (in Hebrew with English Abstract).

Davidson, D. M., Jr. 1980. Emplacement and deformation of the Archean Saganaga batholith, Vermilion District, northeastern Minnesota. *Tectonophysics* **66**, 179–195.

Dixon, J. M. 1975. Finite strain and progressive deformation in models of diapiric structures. *Tectonophysics* **28**, 89–124.

Gaber, L. 1983. The structural petrology of the Wadi Kid—Wadi Beda area (SE Sinai). Unpublished M.Sc. thesis, Ben-Gurion University of the Negev, Beersheva.

Guillet, P., Bouchez, J.-L. & Wagner, J.-J. 1983. Anisotropy of magnetic susceptibility and magmatic structures in the Guerande granite massif (France). *Tectonics* **2**, 419–429.

Halpern, M. & Tristan, N. 1981. Geochronology of the Arabian–Nubian Shield in southern Israel and eastern Sinai. *J. Geol.* **89**, 639–648.

Holder, M. T. 1979. An emplacement mechanism for post-tectonic granites and its implications for the geochemical features. In: *Origin of Granite Batholiths, Geochemical Evidence* (edited by Atherton, M. P. & Tarney, J.). Shiba, U.K., 116–128.

Manktelow, N. S. 1979. The development of slaty cleavage, Fleurieu Peninsula, South Australia. *Tectonophysics* **58**, 1–20.

March, A. 1932. Mathematische Theorie der Regelung nach der Korngestalt bei affiner Deformation. *Z. Kristallographie* **81**, 285–297.

Mattauer, M. 1975. Sur le mechanisme de formation de la schistosité dans l'Himalaya. *Earth Planet. Sci. Lett.* **28**, 144–154.

Morgan, J. 1980. Deformation due to distension of cylindrical igneous contacts: a kinematic model. *Tectonophysics* **66**, 167–178.

Navon, O. & Reymer, A. P. S. 1984. Stratigraphy, structures and metamorphism of Pan-African age in central Wadi Kid area, southeastern Sinai. *Israel J. Earth Sci.* **33**, 135–149.

Nelson, C. A., Oertel, G., Christie, J. M. & Sylvester, A. G. 1977. Geologic Map, structure sections and palinspastic map of Papoose Flat Pluton, Inyo Mountains, California. *Geol. Soc. Am. Map and Chart Series*, MC-20.

Oertel, G. 1981. Strain estimation from scattered observations in an inhomogeneously deformed domain of rocks. *Tectonophysics* **77**, 133–150.

Oertel, G. 1983. The relationship of strain and preferred orientation of phyllosilicate grains in rocks—a review. *Tectonophysics* **100**, 413–447.

Oertel, G. 1985a. Reorientation due to grain shape. In: *Preferred Orientation in Deformed Materials* (edited by Wenk, H. R.). Academic Press, New York, 259–265.

Oertel, G. 1985b. Phyllosilicate textures in slates. In: *Preferred Orientation in Deformed Materials* (edited by Wenk, H. R.). Academic Press, New York, 431–440.

Priem, H. N. A., Eyal, M., Hebeda, E. H. & Verdurmen, E. A. Th. 1984. U–Pb zircon dating in the Precambrian basement of the Arabo-Nubian Shield of the Sinai Peninsula: a progress report. Abstract. Eur. Conf. Geochron. Cosmochron. VII, 1984, *Terra Cognita Spec. Issue*, 30–31.

Ramsay, J. G. 1975. The structure of the Chindamora batholith. Abstract. In: *19th Ann. Rep. Res. Inst. Afr. Geol.* (edited by Coward, M. P.). —University of Leeds, 81.

Rattey, P. R. & Sanderson, D. J. 1984. The structure of SW Cornwall and its bearing on the emplacement of the Lizard Complex. *J. geol. Soc. Lond.* **141**, 87–95.

Reymer, A. P. S. 1983. Metamorphism and tectonics of a Pan-African terrain in southeastern Sinai. *Precambrian Res.* **19**, 225–238.

Reymer, A. P. S. 1985. The origin and microstructures of metamorphic felsic dykes emplaced during brittle–ductile extension (Southeast Sinai). *Geol. Mag.* **122**, 27–38.

Reymer, A. P. S. & Oertel, G. 1982. Progressive rock transformation in a metarhyolite: chemical reactions, strain and micafabric development. Extended Abstract. *Mitt. Geol. Inst. ETH Zürich, Neue Folge* **239a**, 237–240.

Reymer, A. P. S. & Yogev, A. 1983. Stratigraphy and tectonic history of the southern Wadi Kid metamorphic complex. *Israel J. Earth Sci.* **32**, 105–116.

Reymer, A. P. S., Matthews, A. & Navon, O. 1984a. Pressure–temperature conditions in the Wadi Kid metamorphic complex: implications for the Pan-African event in Sinai. *Contr. Miner. Petrol.* **85**, 336–345.

Reymer, A. P. S., Matthews, A. & Avigad, D. 1984b. Inverse metamorphic zonation, thrusting and folding in NE Sinai: evidence for Pan-African crustal shortening. *Abs. with Prog. geol. Soc. Am.* **16**, 633.

Rosenfeld, J. L. 1968. Garnet rotations due to the major Paleozoic deformations in southeast Vermont. In: *Studies of Appalachian Geology: Northern and Maritime* (edited by Zen, E-An, White, W. S., Hadley, J. B. & Thompson, J. B.). Wiley, New York, 185–202.

Schwerdtner, W. M., Sutcliffe, R. H. & Troeng, B. 1978. Patterns of total strain in the crestal region of immature diapirs. *Can. J. Earth Sci.* **15**, 1437–1447.

Schwerdtner, W. M., Stott, G. M. & Sutcliffe, R. H. 1983. Strain patterns of crescentic granitoid plutons in the Archean greenstone terrain of Ontario. *J. Struct. Geol.* **5**, 419–430.

Shimron, A. E. 1980. Proterozoic island arc volcanism and sedimentation in Sinai. *Precambrian Res.* **12**, 437–458.

Shimron, A. E. 1983. The Tarr Complex revisited—folding, thrusts, and mélanges in the southern Wadi Kid region, Sinai Peninsula. *Israel J. Earth Sci.* **32**, 123–148.

Shimron, A. E . 1984. Evolution of the Kid Group, Southeast Sinai Peninsula: thrusts, melanges, and implications for accretionary tectonics during the Late Proterozoic of the Arabian–Nubian Shield. *Geology* **12**, 242–247.

Sibson, R. H. 1983. Continental fault structure and the shallow earthquake source. *J. geol. Soc. Lond.* **140**, 741–767.

Soula, J-C. 1982. Characteristics and mode of emplacement of gneiss domes and plutonic domes in central-eastern Pyrenees. *J. Struct. Geol.* **4**, 313–342.

Sylvester, A. G., Oertel, G., Nelson, C. A. & Christie, J. M. 1978. Papoose Flat Pluton: a granitic blister in the Inyo Mountains, California. *Bull. geol. Soc. Am.* **89**, 1205–1219.

Torske, T. 1982. Structural effects on the Proterozoic Ullensvang Group (West Norway) relatable to forceful emplacement of expanding plutons. *Geol. Rdsch.* **71**, 104–119.

Wenk, H. R. 1985. Measurement of pole figures. In: *Preferred Orientation in Deformed Materials* (edited by Wenk, H. R.). Academic Press, New York, 11–47.

Williams, P. F. & Schoneveld, C. 1981. Garnet rotation and the development of axial plane crenulation cleavage. *Tectonophysics* **78**, 307–334.

Wilson, J. R. 1983. Development of mylonitization during diapirism in the Kettle gneiss dome, Washington. *Abs. with Prog. geol. Soc. Am.* **15**, 719.